Electronic Supplementary Material (ESI) for Inorganic Chemistry Frontiers.

Supporting Information

Dendrite-free solid-state lithium batteries enabled by fluorine doped $Li_7La_3Zr_2O_{12}$ electrolyte and $LiAlF_4$ Interphase

Yuezhen Mao, Fanghui Mi, Tianyuan Wang, Zhijun Zhang, Chunwen Sun,*

School of Chemical & Environmental Engineering, China University of Mining and Technology-Beijing, Beijing 100083, P. R. China.

* Email: csun@cumtb.edu.cn (C. Sun)

Battery Assemblies and Electrochemical Measurements: The stainless steel (SS)/solid electrolyte/SS batteries were assembled to determine ionic conductivities. The electrochemical impedance spectroscopy (EIS) was measured at 25°C using a ZENNIUME electrochemical workstation (Zahner, Germany) in the frequency range from 1M Hz to 0.01 Hz with a perturbation of 10 mV. The electrolyte membranes and garent-type electrolytes are sandwiched between a pair of SS-blocking electrodes. The ionic conductivity (σ) was calculated from the following equation, where R is the resistance value of the bulk electrolyte measured by EIS, and L is the thickness of electrolyte membrane, and S is the area of electrode:

$$\sigma = \frac{L}{RS}$$

Activation energy calculations for the composite solid electrolyte membrane were performed using the Arrhenius formula, where σ denotes the ionic conductivity, L denotes the thickness of the composite solid electrolyte, T is the Kelvin temperature, and R is the molar gas constant 8.314 J mol^{-1} K^{-1}.

$$\sigma = A\exp\left(\frac{-E_a}{RT}\right)$$

The Li^+ transference number of electrolytes were determined by constant potential chronoamperometry combined with EIS, and the Li||xF-LLZO CSE||Li cell were polarized with a DC voltage of 10 mV, and the initial current (I_0) and steady-state current (I_{ss}) flowing through the cell were measured for 6000s. R_0 and R_{SS} are the resistance values before and after the system perturbation, respectively, and they were calculated from the battery impedance spectra in the frequency range of 1 MHz to 1 mHz, and the oscillation voltage is 10 mV. The Li^+ transference number is calculated by the following equation:

$$t_{Li^+} = \frac{I_{ss}(\Delta V - I_0 R_0)}{I_0(\Delta V - I_{ss} R_{ss})}$$

A $LiFePO_4$||Li cells was assembled by sandwiching the as-prepared CSE membranes between metallic lithium and $LiFePO_4$ (LFP) cathode to test their cycling performance on the battery test system (China Land) in a voltage range of 2.6~3.9 V

at room temperature. The cells described above were all assembled in an argon-filled glove box. In order to wet the interface and reduce the interface resistance, 10 μL of electrolyte (1 M $LiPF_6$ in EC: DMC) was added dropwise to the solid–solid contact interface in all batteries.

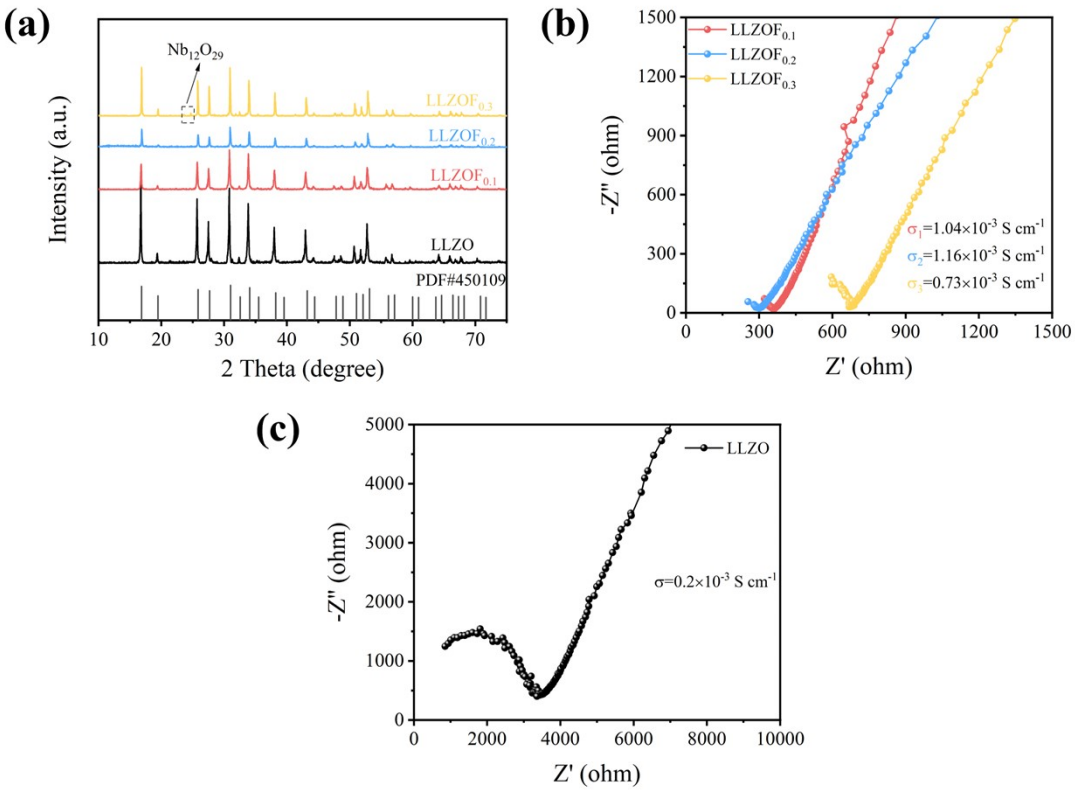

Fig. S1. (a) XRD patterns of garnet-type $LLZOF_x$; (b-c) The ionic conductivity of the garnet-type $LLZOF_x$.

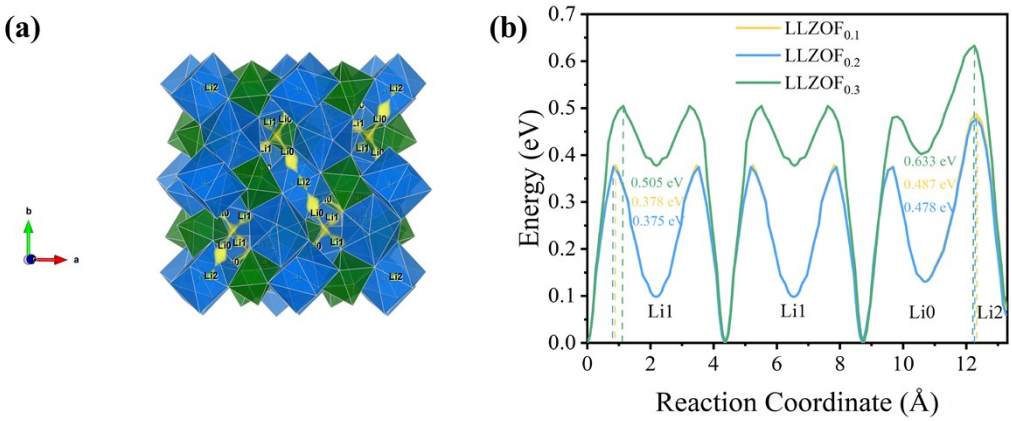

Fig. S2. (a) Schematic image of the yellow channel represents the diffusion path of Li ions in $LLZOF_{0.2}$, and (b) the bond valence site energy (BVSE) of the corresponding migration barrier in three samples[1-3].

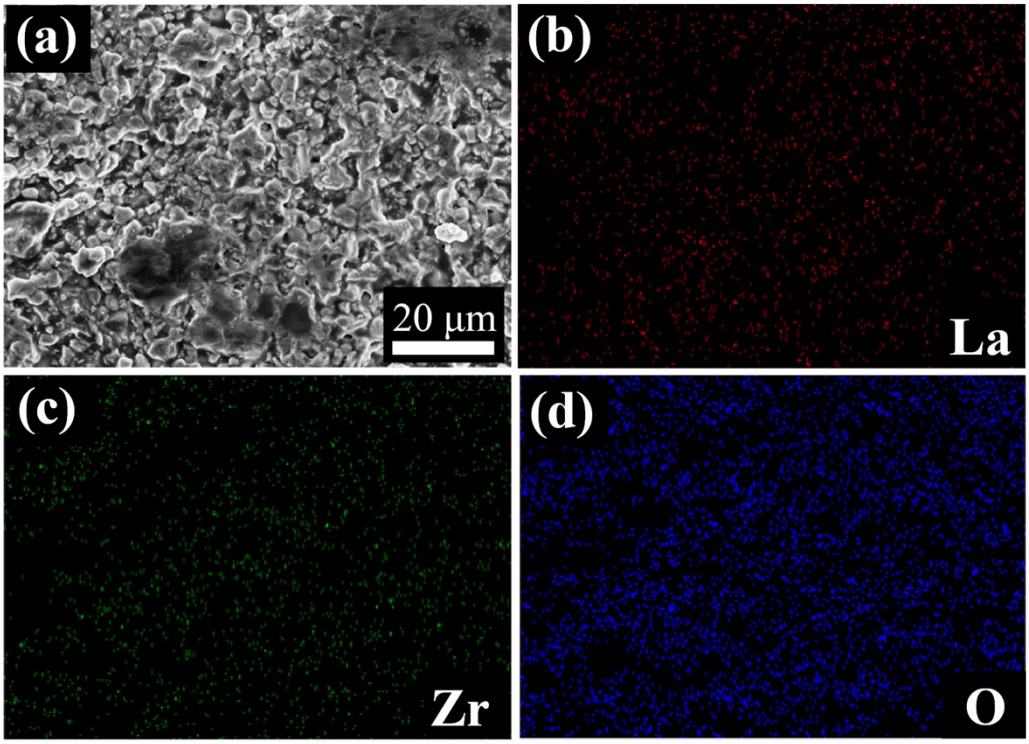

Fig. S3. SEM image (a) and EDS elemental mappings of (b) La, (c) Zr and (d) O in LLZO.

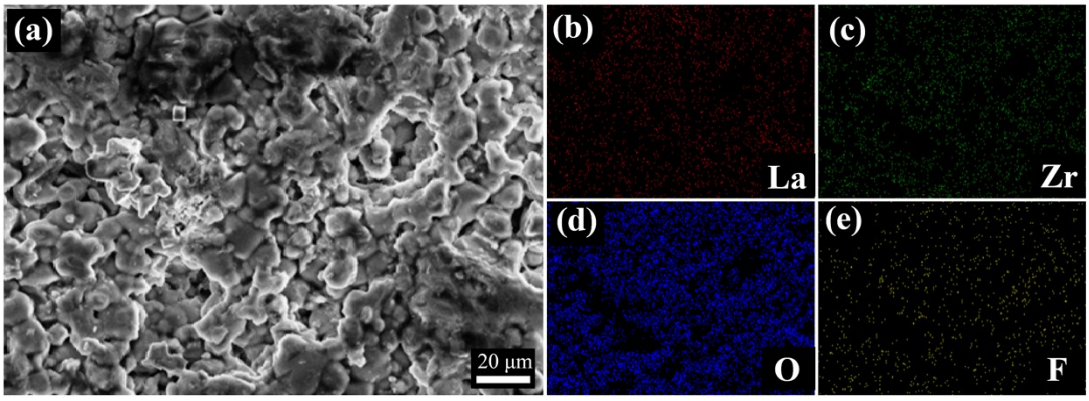

Fig. S4. SEM image (a) and EDS elemental mappings of (b) La, (c) Zr, (d) O and (e) F in $LLZOF_{0.2}$.

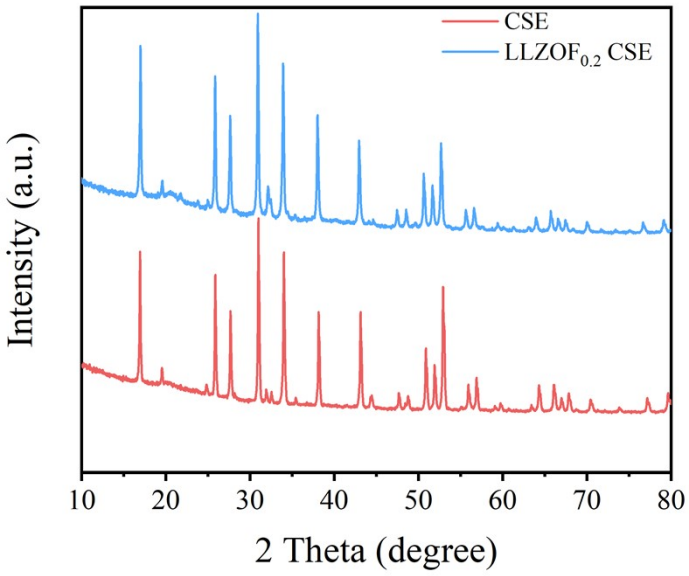

Fig. S5. XRD patterns of CSE and $LLZOF_{0.2}$ based CSE.

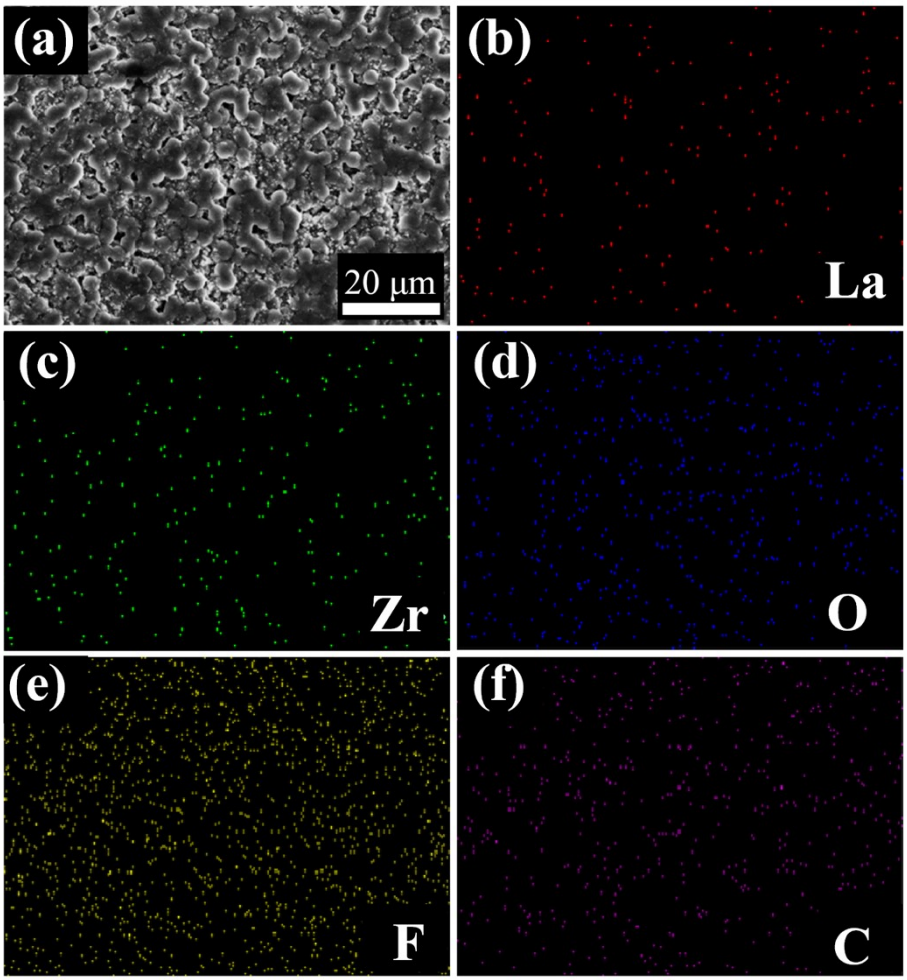

Fig. S6. SEM image (a) and EDS elemental mappings of (b) La, (c) Zr, (d) O, (e) F and (f) C in $LLZOF_{0.2}$ CSE.

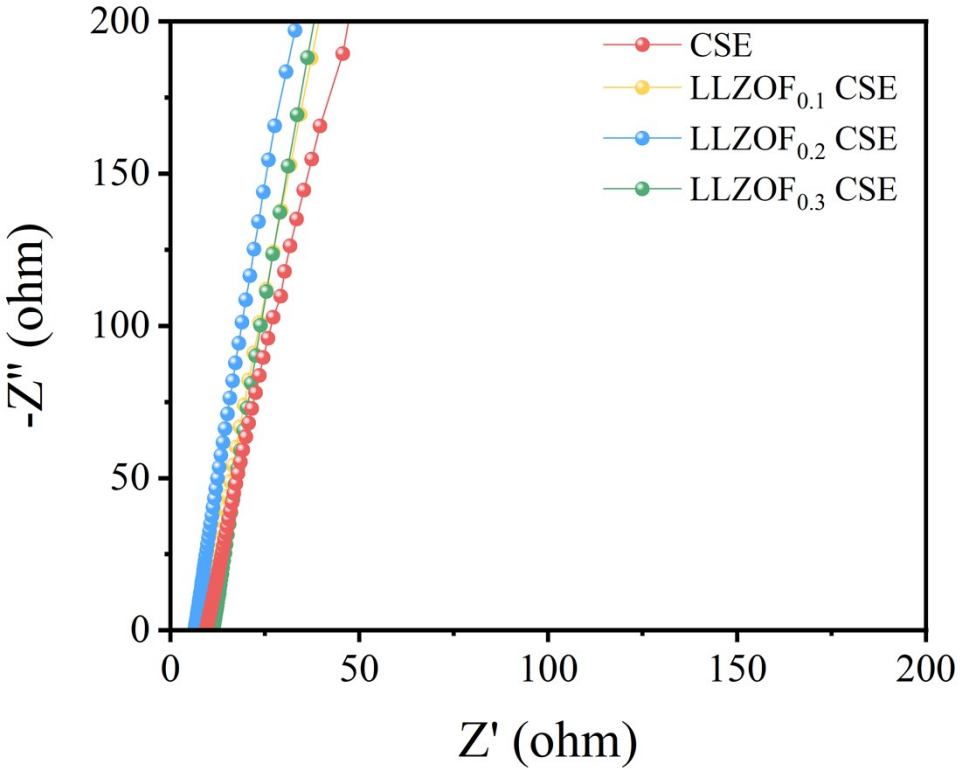

Fig.S7. EIS spectra of SS||SS cells with $LLZOF_x$ CSEs at room temperature.

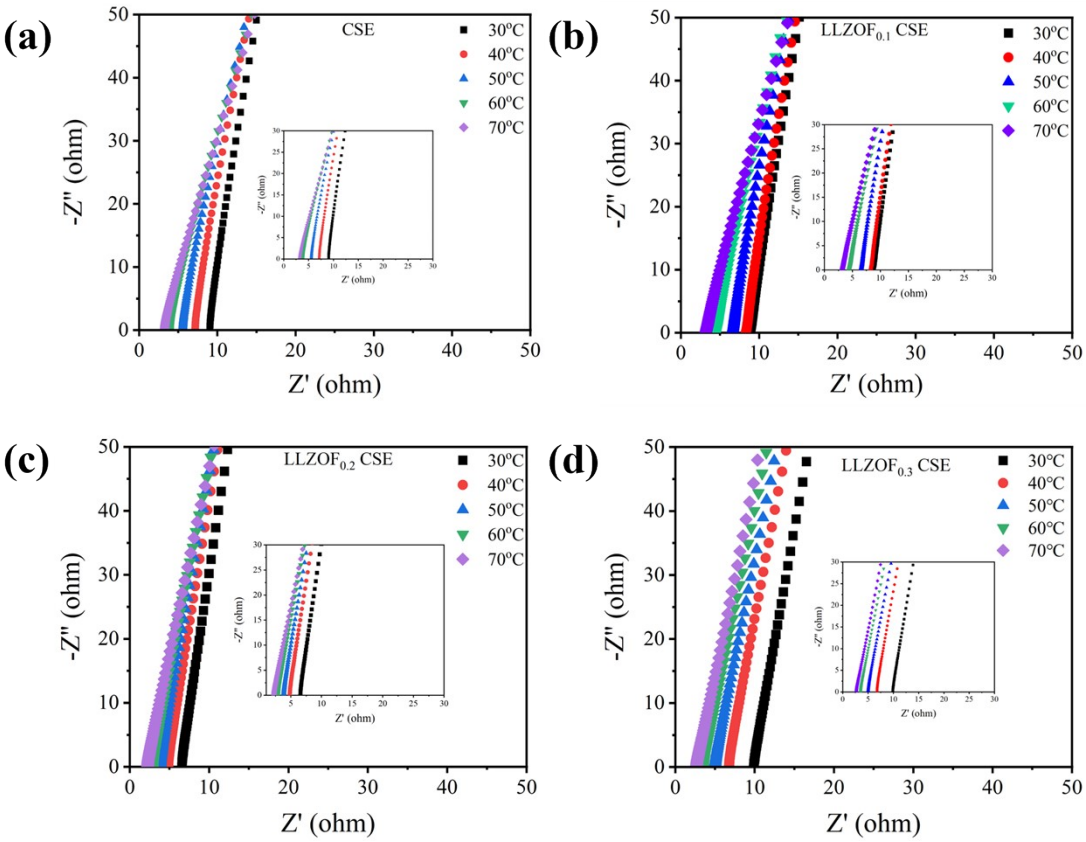

Fig. S8. Ionic conductivities of $LLZOF_x$ CSEs in the range 30-70°C. (a) CSE; (b) $LLZOF_{0.1}$ CSE; (c) $LLZOF_{0.2}$ CSE; (d) $LLZOF_{0.3}$ CSE.

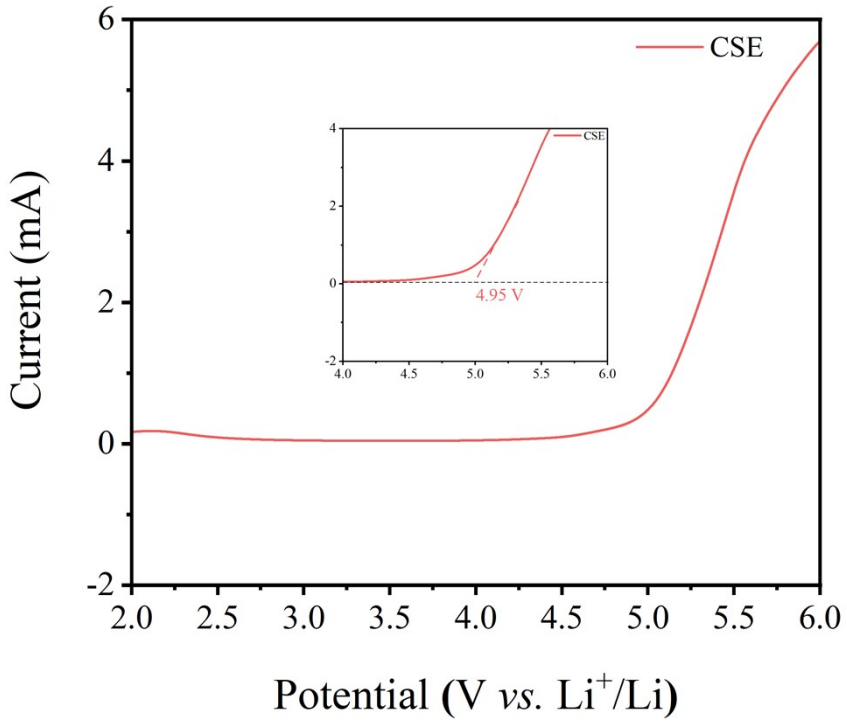

Fig. S9. LSV curve of CSE.

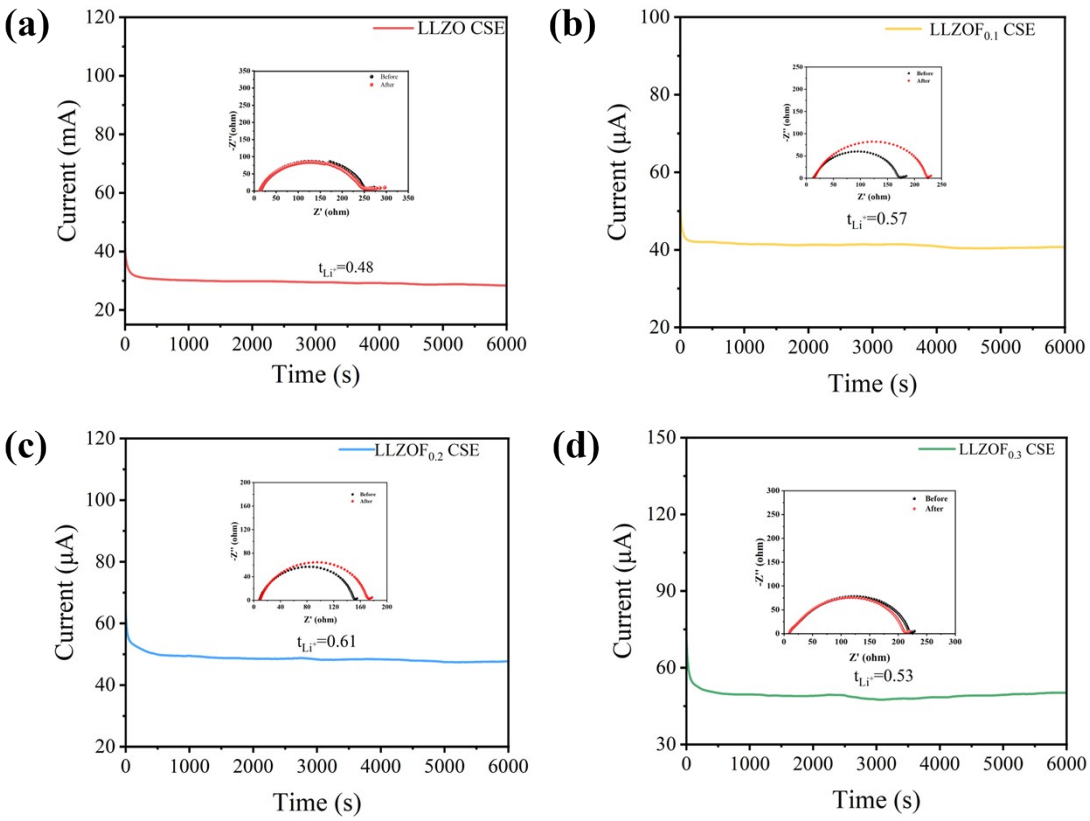

Fig. S10. Current-time profile of the Li||Li symmetric cells after application of 10 mV DC voltage for determination of Li^+ transfer number. The EIS curves of the symmetric cell before and after polarization are shown in the inset. (a) CSE; (b) $LLZOF_{0.1}$ based CSE; (c) $LLZOF_{0.2}$ based CSE; (d) $LLZOF_{0.3}$ based CSE.

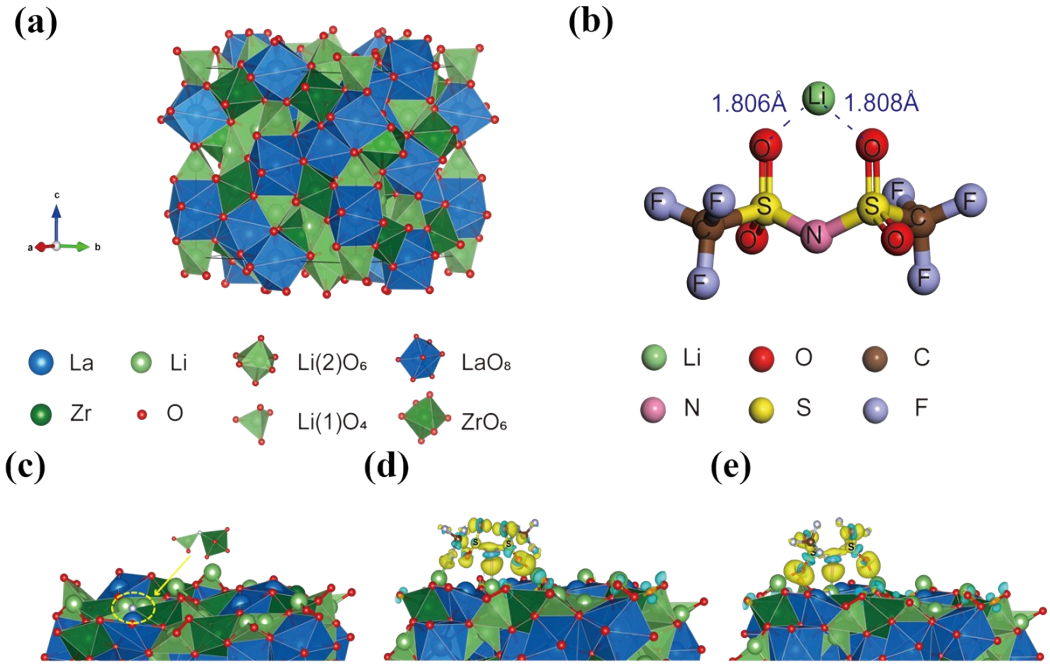

Fig. S11 (a) The model of $Li_7La_3Zr_2O_{12}$. (b) The model of LiTFSI. (c) The model depicts the (110) surface of $LLZOF_{0.2}$ and the atoms circled in yellow is F atom. (d) The Charge transfer at the LLZO (110)-$TFSI^-$ interface. (e) the $LLZOF_{0.2}$ (110)-$TFSI^-$ interface by charge density difference. Yellow and blue indicate charge accumulation and charge depletion, respectively.

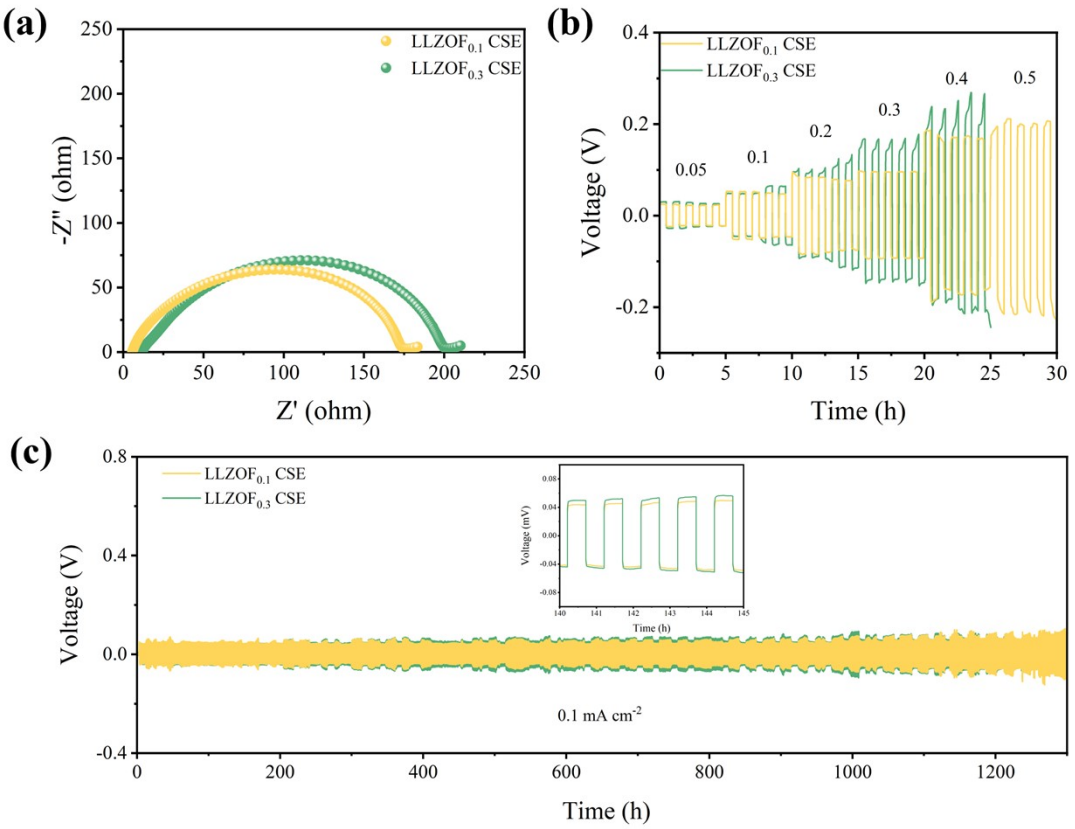

Fig. S12. (a) The interface resistance of Li symmetric cells with $LLZOF_{0.1}$ CSE and $LLZOF_{0.3}$ CSE; (b) The critical current density (CCD) of Li||$LLZOF_{0.1}$ CSE ||Li and Li||$LLZOF_{0.3}$ CSE||Li cell; (c) Voltage profiles of symmetric coin cells at 0.1 mA cm^{-2}, and the inset shows the enlarged voltage profiles of the symmetric cells during 141~145 h.

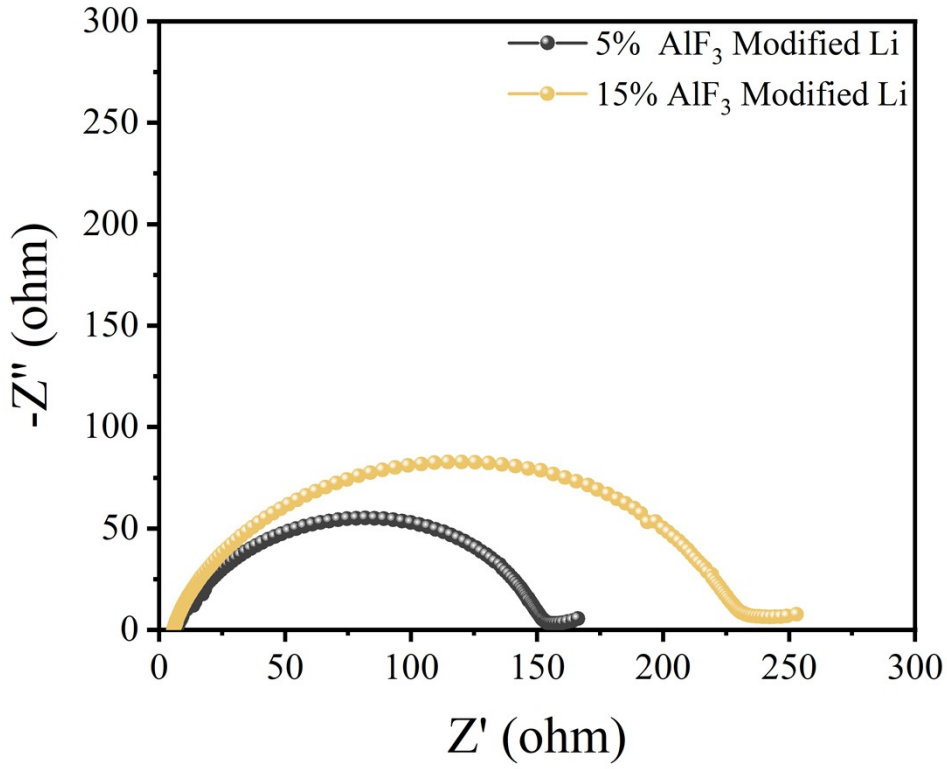

Fig. S13. The interfacial resistance of Li symmetric cells with different concentrations AlF_3 in DMSO solvent.

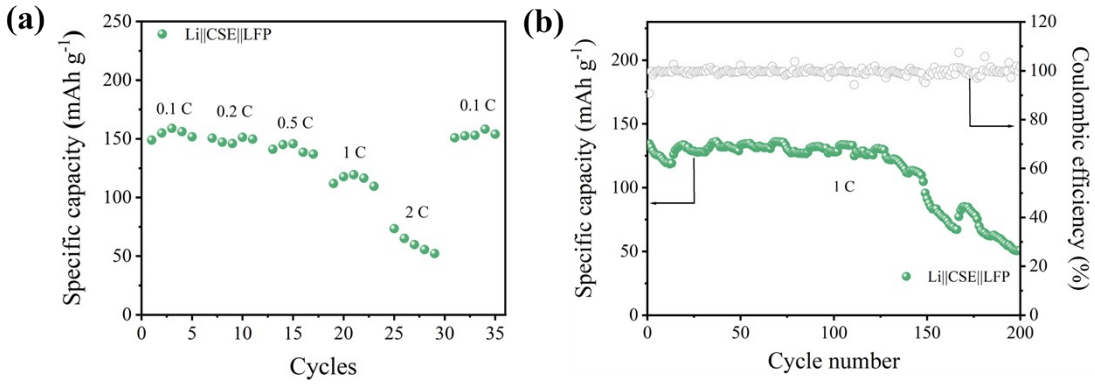

Fig. S14. The rate and cycling performance of Li||CSE||LFP. (a) Rate performance; (b) Cycling performance.

Table S1. A comparison of ionic conductivity of the $LLZOF_{0.2}$ based CSE with composite electrolytes reported in the literatures.

Electrolyte	Ionic conductivity at room temperature	References
SSE-10	1.1×10^{-4} S cm^{-1}	4
PCEs	1.8×10^{-4} S cm^{-1}	5
3D CPE	9.2×10^{-5} S cm^{-1}	6
PDOL/LLZTO	2.9×10^{-4} S cm^{-1}	7
PEGMEM@LLZTO	3.16×10^{-4} S cm^{-1}	8
PLLB	1.16×10^{-4} S cm^{-1}	9
NDCPE-5%	2.9×10^{-4} S cm^{-1}	10
CSE-Ice-60	1.2×10^{-4} S cm^{-1}	11
$LLZOF_{0.2}$ CSE	3.9×10^{-4} S cm^{-1}	This work

References

1. S. Adams and R. P. Rao, High power lithium ion battery materials by computational design, *physica status solidi (a)*, 2011, **208**, 1746-1753.
2. H. Chen and S. Adams, Bond softness sensitive bond-valence parameters for crystal structure plausibility tests, *IUCrJ*, 2017, **4**, 614-625.
3. H. Chen, L. L. Wong and S. Adams, SoftBV-a software tool for screening the materials genome of inorganic fast ion conductors, *Acta Crystallogr B Struct Sci Cryst Eng Mater*, 2019, **75**, 18-33.
4. J. Yu, S. C. T. Kwok, Z. Lu, M. B. Effat, Y. Q. Lyu, M. M. F. Yuen and F. Ciucci, A ceramic-PVDF composite membrane with modified interfaces as an ion-conducting electrolyte for solid-state lithium-ion batteries operating at room temperature, *ChemElectroChem*, 2018, **5**, 2873-2881.
5. Z. Li, H.-X. Xie, X.-Y. Zhang and X. Guo, In situ thermally polymerized solid composite electrolytes with a broad electrochemical window for all-solid-state lithium metal batteries, *Journal of Materials Chemistry A*, 2020, **8**, 3892-3900.
6. S. Song, X. Qin, Y. Ruan, W. Li, Y. Xu, D. Zhang and J. Thokchom, Enhanced performance of solid-state lithium-air batteries with continuous 3D garnet network added composite polymer electrolyte, *Journal of Power Sources*, 2020, **461**, 228146-228152.
7. L. X. Li, R. Li, Z. H. Huang, H. Yang, M. Q. Liu, J. Xiang, S. Hussain, X. Q. Shen and M. X. Jing, A multifunctional gradient solid electrolyte remarkably improving interface compatibility and ion transport in solid-state lithium battery, *ACS Applied Materials & Interfaces*, 2022, **14**,

30786-30795.
8. Z. Gu, X. Xin, Z. Xu, J. He, J. Wu, Y. Sun and X. Yao, Garnet electrolyte-based integrated architecture for high-performance all-solid-state lithium-oxygen batteries, *Advanced Functional Materials*, 2023, **33**, 2301583-2301593.
9. C. Lei, J. Li, Z. Tan, Y. Li, P. He, Y. Liu, Y. Li, F. Wu, Y. Cheng and Z. He, Double-layer electrolyte boosts cycling stability of all-solid-state li metal batteries, *ACS Applied Materials & Interfaces*, 2023, **15**, 31572-31583.
10. S. Lv, X. He, Z. Ji, S. Yang, L. Feng, X. Fu, W. Yang and Y. Wang, A supertough and highly-conductive nano-dipole doped composite polymer electrolyte with hybrid Li^+-solvation microenvironment for lithium metal batteries, *Advanced Energy Materials*, 2023, **13**, 2302711-2302725.
11. R.-J. Pei, Y.-F. Li, T. Song, N. Chen and R. Yang, A solid composite electrolyte of 3D framework $Li_{6.25}La_3Sn_{1.25}Bi_{0.75}O_{12}$ for rechargeable solid-state batteries, *Journal of Alloys and Compounds*, 2023, **933**, 167639-167648.